



139
207
THS

**LIBRARY
Michigan State
University**

This is to certify that the
thesis entitled


CHARACTERIZATION OF *E. coli* Aid B: A COMPONENT OF THE
ADAPTIVE RESPONSE TO ALKYLATING AGENTS

presented by

Mukta S. Rohankhedkar

has been accepted towards fulfillment
of the requirements for the

Masters degree in Cell and Molecular Biology



Major Professor's Signature

Oct. 11, 2005

Date

PLACE IN RETURN BOX to remove this checkout from your record.
TO AVOID FINES return on or before date due.
MAY BE RECALLED with earlier due date if requested.

DATE DUE	DATE DUE	DATE DUE

**CHARACTERIZATION OF *E. coli* Aid B: A COMPONENT OF THE ADAPTIVE
RESPONSE TO ALKYLATING AGENTS**

By

Mukta S. Rohankhedkar

A THESIS

**Submitted to
Michigan State University
in partial fulfillment of the requirements
for the degree of**

MASTER OF SCIENCE

Cell and Molecular Biology Program

2005

ABSTRACT

CHARACTERIZATION OF *E. coli* Aid B: A COMPONENT OF THE ADAPTIVE RESPONSE TO ALKYLATING AGENTS.

By

Mukta S. Rohankhedkar

Upon exposure to alkylating agents, *Escherichia coli* increases expression of *aidB* along with three genes (*ada*, *alkA*, and *alkB*) that encode DNA-repair proteins. In order to begin to identify the role of AidB in the cell, the protein was purified to homogeneity, shown to possess stoichiometric amounts of FAD, and confirmed to have low levels of isovaleryl-CoA dehydrogenase activity. A homology model of an AidB homodimer was constructed based on the structure of a four-domain acyl-CoA oxidase; the predicted structure revealed a positively charged groove connecting the two active sites and a second canyon of positive charges in the C-terminal domain, both of which could potentially bind DNA. Three approaches were used to confirm that AidB binds to DNA, and the protein has slightly greater affinity for MNNG-treated (alkylated) dsDNA. On the basis of its ability to bind DNA and its possession of a redox-active flavin, AidB is predicted to catalyze the direct repair of alkylated DNA.

ACKNOWLEDGEMENTS

I would like to thank my advisor Dr. Robert Hausinger for his invaluable guidance and support. His dedication to his students and encouraging nature has helped me become an independent thinker. I would like to thank my committee members Dr. Kathy Meek, Dr. Zach Burton and Dr. Kathy Gallo for all their contributions towards the completion of this thesis. Special thanks to Dr. William Wedemeyer for his contributions with the AidB modeling studies. I owe a great deal to all the help I have received from my lab mates: Dr. Scott Mulrooney for helping me from the first day of my rotation to the day that I finished doing my last experiment in the lab and even with editing this thesis, Tina and Kim for their scientific input and words of encouragement when things were not going so great and for all the fun that we had at the aerobics classes, Soledad, Piotr, Thalia, Meng and Jana for always being encouraging and making the lab a great place to work.

I would like to thank all my friends in East Lansing especially Soumya and Tejas for always being there for me and helping me find a home away from home. I am especially thankful to my parents, my sister and my brother for always being supportive and encouraging me to do the best I can. Finally I would like to thank my husband Sachin Vaidya for always bringing out the best in me. His constant love support and encouragement have made me a better scientist and a better person.

TABLE OF CONTENTS

LIST OF FIGURES	V
LIST OF SCHEMES	VI
INTRODUCTION.....	1
MECHANISMS OF DNA DAMAGE:.....	2
MECHANISMS OF DNA REPAIR:	6
THE ADAPTIVE RESPONSE PROTEIN AIDB.	14
FOCUS OF THIS THESIS.	17
CHARACTERIZATION OF THE AID B COMPONENT OF THE <i>E. COLI</i>	
ADAPTIVE RESPONSE TO METHYLATING AGENTS.	18
MATERIALS AND METHODS	21
<i>Cloning and expression of aidB.</i>	21
<i>Purification of AidB.</i>	22
<i>Native molecular weight of AidB</i>	22
<i>Characterization of the AidB cofactor.</i>	23
<i>Isovaleryl-CoA dehydrogenase activity assay.</i>	24
<i>DNA binding assays.</i>	24
<i>Sequence analysis and homology modeling</i>	26
RESULTS	27
<i>Purification of AidB</i>	27
<i>Biophysical characterization of AidB</i>	27
<i>Enzymatic characterization of AidB.</i>	33
<i>DNA binding by AidB.</i>	33
<i>Sequence analysis and homology modeling</i>	37
DISCUSSION	43
<i>Characterization of AidB as a flavin-containing isovaleryl-CoA dehydrogenase....</i>	43
<i>Identification of AidB as a DNA-binding protein.</i>	44
<i>Quaternary structure of AidB.</i>	44
<i>Predicted structure of AidB.</i>	45
<i>Potential cellular function of AidB.</i>	46
CONCLUSIONS AND FUTURE DIRECTIONS.....	48
REFERENCES.....	54

LIST OF FIGURES

Figure 1.1: DNA damage as a result of external damaging agents.....	4
Figure 1.2: DNA methylating agents.....	5
Figure 1.3: Base excision pathway for DNA repair.....	8
Figure 1.4: Nucleotide excision repair pathway for DNA repair.....	9
Figure 1.5: Mismatch repair pathway.....	10
Figure 1.6: Ada mediated response to DNA methylation.....	12
Figure. 2.1: SDS-PAGE analysis of AidB purification.....	28
Figure 2.2: Dithionite titration of AidB.....	31
Figure 2.3: Photoreduction of AidB.....	32
Figure 2.4: Binding of AidB to DNA cellulose.....	34
Figure 2.5: DNA-induced protection against protease digestion of an AidB domain.....	35
Figure 2.6: AidB-induced mobility shift of dsDNA.....	36
Figure 2.7: Homology model of AidB.....	39
Figure 3.1: Crystals of AidB.....	53

LIST OF SCHEMES

Scheme 2.1: Hypothetical function of AidB.....	47
---	-----------

LIST OF ABBREVIATIONS

MNNG	N-Methyl-N'-Nitro-N-Nitrosoguanidine
MMS	Methylmethane Sulphonate
<i>E. coli</i>	Escherichia coli
BER	Base Excision Repair
NER	Nucleotide Excision Repair
MMR	Mismatch Repair
DNA	Deoxyribonucleic acid
A	Adenine
T	Thiamine
G	Guanine
C	Cytosine
Me	Methyl
MI	Methyl Iodide
α KG	Alpha ketoglutarate
TBE	Tris-borate EDTA
TB	Terrific Broth
TCEP	Tris 2-carboxyethyl phosphine
SDS PAGE	Sodiumdodecyl sulfate Polyacrylamide Gel electrophoresis
IPTG	Isopropyl-beta-D-thiogalactopyranoside
MALDI	Matrix assisted laser desorption/ionization technique
DHB	2,5-dihydroxybenzoic acid
FAD	Flavin Adenine Dinucleotide
MCS	Multiple Cloning Site
UV	Ultraviolet
CoA	Coenzyme A
meG	methyl guanine
meA	methyl adenine
meT	methyl thymine

meC	methyl cytosine
5-OhdU	5-hydroxydeoxyuridine
5-OhdC	5-hydroxydeoxycytidine
8-OhdG	8-hydroxydeoxyguanine
8-OhdA	8-hydroxy-deoxyadenine
ss	single stranded
ds	double stranded
AP	apurinic/apyrimidinic

CHAPTER 1

INTRODUCTION

This thesis focuses on the characterization of AidB, an *Escherichia coli* protein thought to function in cellular protection against alkylating agents. As an introduction to my studies, described in chapters 2 and 3, this chapter describes the general mechanisms of damage to deoxyribonucleic acid (DNA), summarizes the cellular mechanisms of DNA repair including a process known as the adaptive response, and provides background information on AidB.

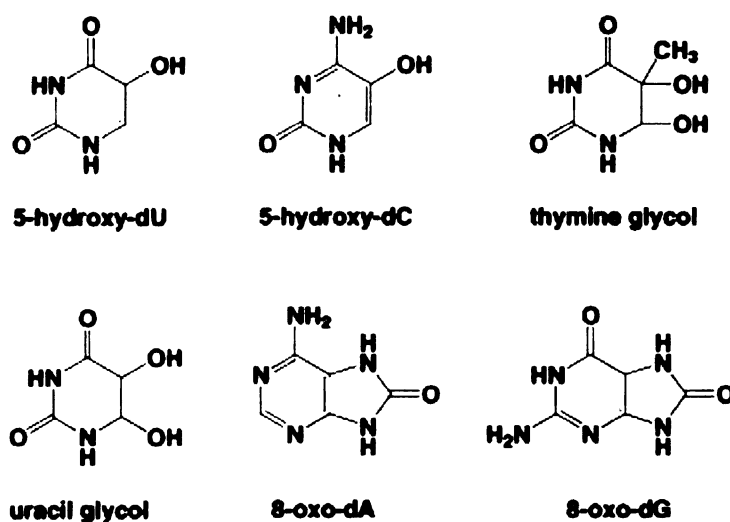
Mechanisms of DNA damage:

The DNA of all living organisms is constantly exposed to endogenously produced and externally derived damaging agents (49). For example, oxygen reacts with flavin-containing electron carriers in the respiratory chain of *E. coli* to produce superoxide anion (O_2^-) and hydrogen peroxide (H_2O_2) at rates estimated to be $5 \mu M \cdot s^{-1}$ and $14 \mu M \cdot s^{-1}$ (17). The H_2O_2 produced is especially deleterious because it reacts with ferrous ions in the cell to produce hydroxyl radicals ($\cdot OH$), which can damage DNA in many ways including strand breakage, formation of abasic sites, and base modifications (described below). In addition to various types of oxidative damage, DNA can be modified by reactive compounds produced in the cell such as *S*-adenosylmethionine, a cellular methylating agent. In addition to the harmful reactions associated with these endogenous compounds, a wide variety of environmental agents can damage DNA as described in the following paragraphs.

Several types of radiation can lead to DNA damage (54). Ultraviolet (UV)-A and UV-B radiation, reaching the earth's surface from the sun, are known to dimerize the rings of adjacent thymines and lead to the formation of cyclopymidine dimers. While

both UV-A and UV-B radiation are directly absorbed by biomacromolecules such as proteins and nucleic acids, UV-A radiation also can lead to the formation of reactive oxygen species (ROS), which can be mutagenic to the DNA. Ionizing radiation such as X rays and gamma rays lead to the direct ionization of the DNA bases, causing single-stranded (ss) or double-stranded (ds) breaks in addition to producing free radicals. Oxidative damage to pyrimidine residues leads to the formation of thymine glycol, uracil glycol, 5-hydroxydeoxyuridine (5-OHdU), and 5-hydroxydeoxycytidine (5-OHdC). Similarly, interaction of $\cdot\text{OH}$ with purines will generate 8-hydroxydeoxyguanine (8-OHdG), 8-hydroxy-deoxyadenine (8-OHdA), and formamidopyrimidines (Figure 1.1)

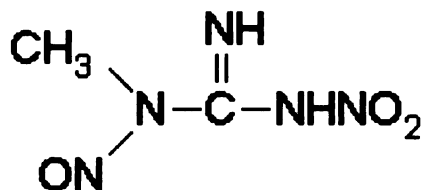
Various chemical mutagens are well known for their ability to cause direct or indirect damage to DNA and RNA (19). Base analogues such as bromouracil, which resembles thymine, and aminopurine, an analog of adenine, can cause potentially toxic A:T to G:C or G:C to A:T transitions in the DNA. Intercalating agents such as ethidium bromide and acridine orange can insert themselves in between DNA bases, thus causing the DNA to stretch and leading to frame shift mutations upon replication. Alkylating agents such as methyl methane sulfonate (MMS), 4-(methylnitrosamino)-1-(3-pyridyl)-1-butanone, 4-(methylnitrosamino)-1-(3-pyridyl)-1-butanol, *N'*-nitrosonornicotine, *N*-methyl-*N'*-nitro-*N*-nitrosoguanidine (MNNG), *N*-methyl-*N*-nitrosourea (MNU) and methyl iodide (MI) are well known for their ability to damage DNA. Alkylation can cause both cytotoxic lesions which block replication and mutagenic lesions that lead to heritable mutations in DNA. DNA methylating agents can react with the N and O atoms of dsDNA (Figure 1.2) resulting in 7-methylguanine (7-meG), 3-methyladenine (3-meA), and O⁶-methylguanine (6-meG) as the most common lesions.



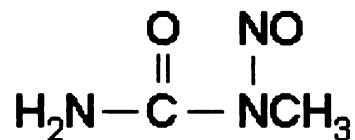
(From: http://www.dojindo.com/newsletter/review_vol2.html)

Figure 1.1: DNA damage as a result of external damaging agents. Various environmental and cellular agents lead to damage to DNA bases. These bases if left unrepaired, can cause cytotoxic and mutagenic lesions in the DNA.

S_N1 type of DNA methylating agents



N-Methyl-*N'*-Nitro-*N*-Nitrosoguanidine
(MNNG)



N-nitroso-N methylurea
(MNU)

S_N2 type of DNA methylating agents



Methyl methane sulphonate



Methyl iodide

Figure 1.2: DNA methylating agents. Based on their reaction mechanism, DNA methylating agents are classified as S_N1 (MNNG, MNU) or S_N2 (MMS, MI) type alkylating agents.

In ssDNA the most common lesions are 1-methyladenine (1-meA) and 3-meC. 1-meA, 3-methylcytosine (3-meC), 3-meA, and 3-methylguanine (3-meG) are cytotoxic and thereby block replication, whereas 6-meG and O⁴-methylthymine (4-meT) cause mutations. Based on their mechanism of action, alkylating agents are classified as S_N1 type, such as MNNG and MNU that introduce an alkyl group at both the N and O atoms in DNA, or S_N2 type, such as MMS and MI that primarily introduce an alkyl group at the N atoms in DNA.

Mechanisms of DNA repair:

The cell employs many mechanisms to repair DNA damage to maintain the integrity of the genetic information that is passed on to the daughter cells (4). These include the key repair pathways such as base excision repair (BER), nucleotide excision repair (NER), mismatch repair (MMR), and, of greatest relevance to this thesis, the adaptive response to DNA damage.

BER (Figure 1.3) is the principle pathway for the repair of oxidatively damaged DNA (28). Enzymes in this pathway recognize DNA lesions such as abasic sites, deaminated cytosine and adenine, and individual bases damaged by oxidative intermediates or alkylating agents. This pathway is initiated by a DNA glycosylase which cleaves the N-glycosidic bond between the target base and the deoxyribose, releasing a free base and leaving an apurinic/apyrimidinic (AP) site. The damaged DNA strand is then cleaved upstream of this AP site by an AP endonuclease to create a 3'-OH terminus adjacent to the AP site. A DNA polymerase then extends this 3'-OH terminus and a DNA ligase finally seals the DNA fragments to complete the repair process.

The NER pathway (Figure 1.4) begins with the initial recognition of the lesion by the UvrA-UvrB complex which tracks along the DNA backbone looking for lesions (62). The UvrA dimer in this complex is responsible for recognizing and binding to damage on dsDNA. The binding of the UvrA dimer to the DNA activates the UvrB helicase activity and leads to the unwinding of the DNA. The conformational change caused by the binding of UvrB to the DNA causes the dissociation of the UvrA dimer, which leads to the binding of UvrC protein. UvrB then initiates the incision of the DNA about 5 bases 3' to the lesion, followed by another incision located 8 bases 5' to the lesion by UvrC. The oligomer thus formed is dissociated by the subsequent binding of the UvrD helicase protein making the site accessible to repair by specific DNA polymerases and ligases, which complete the repair process.

The MMR pathway (Figure 1.5) is involved in the repair of newly synthesized DNA in prokaryotes. The process is initiated by the MutS protein, which recognizes mismatched bases (53). The MutL homodimer is recruited to the DNA-MutS complex in an ATP dependent reaction. The MutH protein binds to this complex, causing the DNA to form a looped structure. The MutH protein recognizes the hemi-methylated GATC sequence in the complex and introduces a nick 5' to the unmethylated GATC sequence of the daughter strand containing the lesion. This nick is then further degraded beyond the site of the mismatch by exonucleases (exonuclease VII for a 5' nick and exonuclease I for a 3' nick), and the DNA strand is repaired by the action of the appropriate polymerases and ligases.

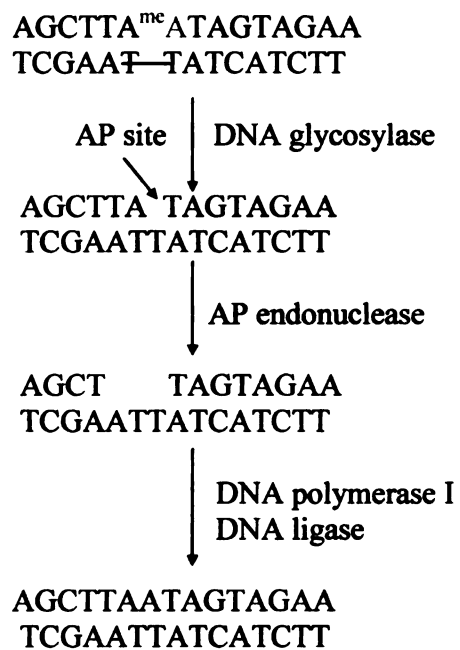


Figure 1.3: Base excision pathway for DNA repair. The damaged base is recognized and excised by a DNA glycosylase to create an apurinic/apyrimidinic site (AP site). The DNA is further cleaved upstream of the AP site by an AP endonuclease to create a 3'-OH terminus which is then extended by a DNA polymerase. A DNA ligase then seals the gap and the strand is repaired.

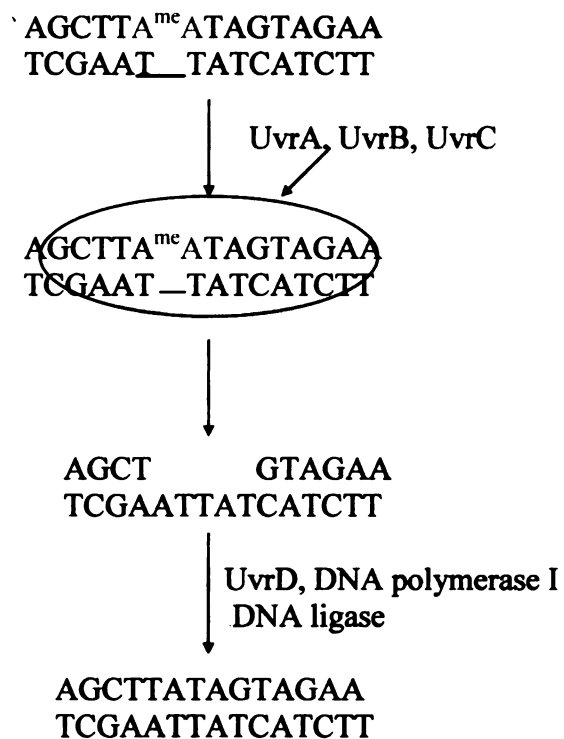


Figure 1.4: Nucleotide excision repair pathway for DNA repair. The lesion in the DNA is recognized by the UvrA-UvrB complex. Binding to DNA causes UvrA to dissociate. The UvrB and UvrC proteins then cleave the DNA 3' and 5' to the site of the damage. The oligomer thus formed is dissociated by the subsequent binding of the UvrD helicase protein making the site accessible to repair by specific DNA polymerases and ligases, which complete the repair process.

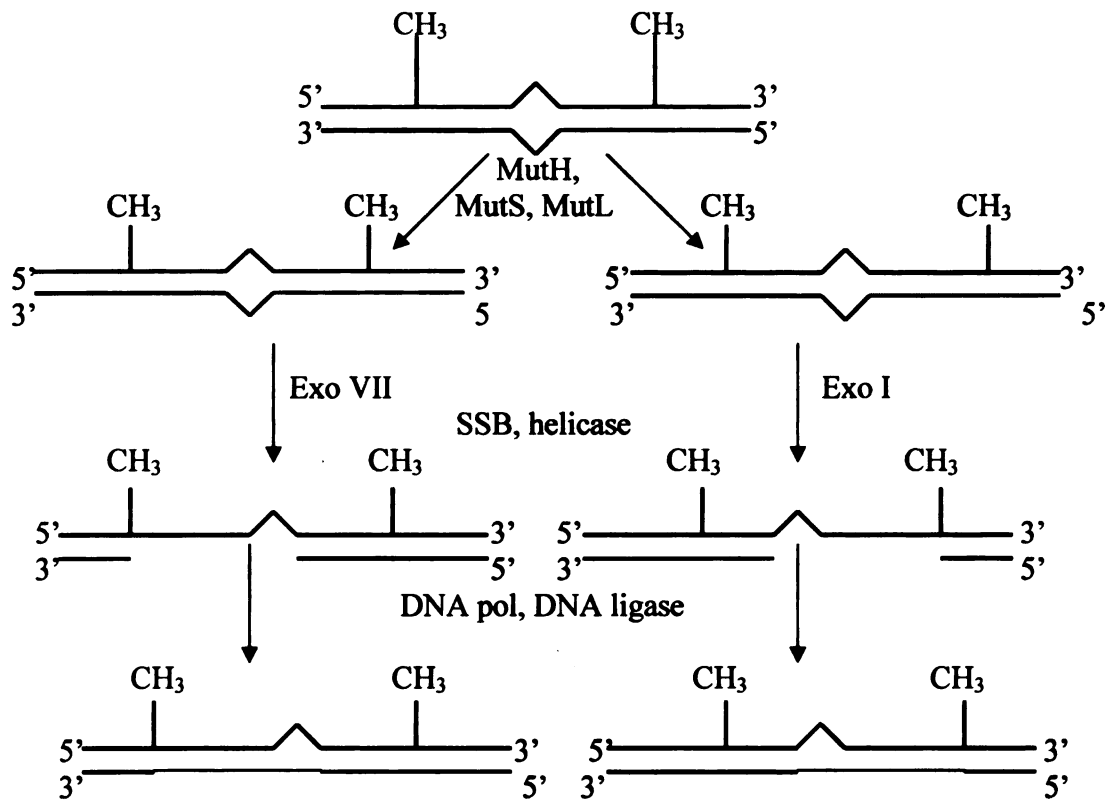


Figure 1.5: Mismatch repair pathway. The process is initiated by the MutS protein, which recognizes mismatched bases (53). The MutL homodimer is recruited to the DNA-MutS complex in an ATP dependent reaction. The MutH protein binds to this complex, causing the DNA to form a looped structure. The MutH protein recognizes the hemimethylated GATC sequence in the complex and introduces a nick 5' to the unmethylated GATC sequence of the daughter strand containing the lesion. This nick is then further degraded beyond the site of the mismatch by exonucleases (exonuclease VII for a 5' nick and exonuclease I for a 3' nick), and the DNA strand is repaired by the action of the appropriate polymerases and ligases.

An important system involved in the protection of DNA against damage caused by alkylating agents involves the “adaptive response” pathway (57, 63, 64, 67, 68) (Figure 1.6). The most important member of this pathway is the Ada protein. Ada is a methyltransferase (20, 51, 56) with two distinct domains, and is capable of transferring methyl groups from DNA onto two specific cysteine residues in its sequence. When the protein encounters 6-meG or 4-meT, it irreversibly transfers the methyl group onto the Cys-321 residue in its carboxyl terminal domain. This is a single turnover reaction, with the protein becoming inactivated as it is methylated at this position. In addition to this carboxyl terminal domain activity, the Ada transfers the methyl group of methylated phosphate triesters to the Cys-38 residue in its amino terminal domain. Methylated phosphate groups are not highly mutagenic but indicate abnormal methylation activity in the DNA. When Ada is methylated at Cys-38 (indicated by ^{me}Ada), it acts as a transcription factor that binds to the promoter regions of three genes making them accessible to transcription by RNA polymerases (60). Methylation at this position is thought to induce a conformational change in Ada and convert it into an active transcription factor. The 3 promoters at which ^{me}Ada acts are those encoding Ada (in a two-gene operon with AlkB), AlkA, and AidB proteins. These proteins are responsible for the repair of methylated DNA.

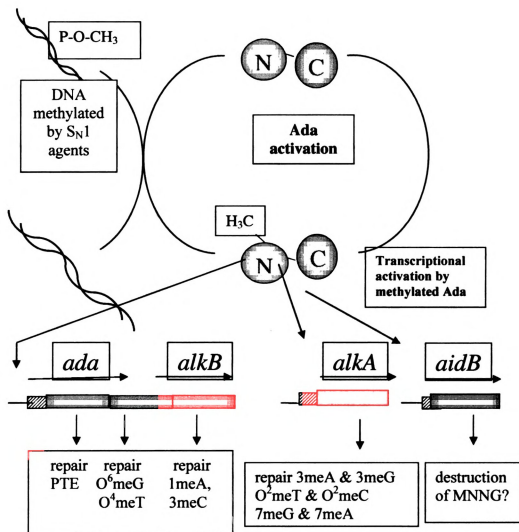


Figure 1.6: Ada mediated response to DNA methylation. Ada transfers the methyl group from methylphosphotriesters onto the Cys-38 residue and in the ^{me}Ada form can activate the transcription of *ada*, *alkA*, *alkB* and *aidB*.

Activation of *ada/alkB* and *aidB* is achieved by similar mechanisms (34). The amino terminal domain of ^mAda binds to the UP promoter element in the promoter regions, independent of RNA polymerase. Initial binding is followed by the interaction of the carboxyl terminal domain of ^mAda with the σ subunit of RNA polymerase, mediated by a patch of negatively charged residues in the σ^{70} subunit of RNA polymerase. This interaction in turn leads to the formation of a stable ternary complex required for the initiation of transcription. Structural data indicate that Cys-321 and its surrounding amino acids are buried in the interior of the protein and not accessible to solvent. Upon binding to DNA the protein undergoes a conformational change that exposes these residues, and methylation of Cys-321 stabilizes this conformation. Thus, methylation of Cys-321 is required for optimal ^mAda-mediated transcription.

In the case of the *alkA* promoter, the ^mAda binding site is located such that its amino terminal domain can simultaneously interact with both the σ^{70} subunit of the RNA polymerase as well as its α -carboxyl terminal domain. Unmethylated Ada is capable of activating the *alkA* promoter weakly but cannot do the same at the promoters of *ada/alkA* and *alkB*. Although the transcriptional activation of *alkA*, *alkB* and *aidB* is similar, their protein products act in very different ways to repair methylated DNA.

AlkA is an alkyl base glycosylase which acts mainly on the 3-meA and 3-meG residues in DNA. It binds to the DNA and flips out the nucleotide substrate to expose it to the enzyme's active site (15). The enzyme active site is filled with electron-rich residues, which explain its specificity towards electron-deficient damaged bases. The enzyme removes the methylated base from the DNA creating an abasic site, which is acted upon

by an AP endonuclease, a repair specific DNA polymerase, and a ligase to complete the repair process.

AlkB is an Fe(II)- and α -ketoglutarate dependent dioxygenase that repairs 1-meA and 3-meC lesions (61). In the presence of Fe(II) and α -ketoglutarate, it oxidatively decarboxylates α -ketoglutarate to form succinate while hydroxylating the methyl group in these bases to create an intermediate that spontaneously releases formaldehyde from the repaired bases. AlkB acts on both ssDNA and dsDNA, though its efficiency is much higher with the former. Several human homologues of AlkB have recently been identified (1, 70), but their functions are still not completely clear.

The Adaptive Response Protein AidB.

As opposed to Ada, AlkA and AlkB, very little information is available about the role and mechanism of action of AidB. The gene was identified as a part of the adaptive response to methylating agents and is induced by Ada (63, 67, 68). In these studies, random insertions were made using Mu dl(Ap^Rlac) and the resulting mutants were selected such that β -galactosidase synthesis was under the control of genes whose promoters were induced in response to treatment with MMS and MNNG. It was observed that some of the mutant cells had increased resistance to the methylating agent MNNG, while other derivative strains exhibited increased resistance to MNNG but not to other methylating agents (33). This surprising result might be due to enhanced activity or stabilization of the protein in these constructs where the sites of insertion were localized to the 3' region of the gene. However the exact positions of the insertions are unclear.

AidB was also reported to be induced by anaerobiosis (65) and acidification of the cytoplasm (59). As in the above-mentioned experiments, insertional mutants were used for these studies. Strains containing fusions of *aidB::Mu dl(bla lac)* were used to test induction of *aidB* by monitoring the β -galactosidase activity in the cell extracts of anaerobically grown cells (65). β -galactosidase activity remained low in the aerated culture, but *aidB::Mu dl(bla lac)* was induced to high levels in the unaerated culture. However, the exact location of this insertion was unclear, as was the reason for the observed increase in expression. It was also noted that the expression of *aidB* under anaerobic conditions is mediated by *rpoS* (66), a gene which encodes an alternative sigma factor of RNA polymerase which is mainly active in late exponential and stationary phases of *E. coli* growth.

In another study, random insertions of mini-Tn10(Kan^r) were introduced via P1-mediated transduction into the bacterial strain MV2450 containing an *aidB-lacZ* operon fusion to detect mutations affecting *aidB* expression under anaerobic conditions (42). These experiments indicated that anaerobic induction of *aidB* requires the presence of a functional *cysA* operon encoding a sulfate permease. The functional significance of this finding is still unclear.

Cloning of *aidB* was performed in two steps using the *aidB::Mu dl(bla lac)* fusion strain, which yielded all the regulatory sequences and upstream promoters of *aidB*, while the rest of the gene was subcloned from λ 654(λ IG10) of the Kohara collection (33). DNA sequencing yielded an open reading frame of 1642 nucleotides with a putative protein product of 60.5 kDa. It was also demonstrated that cells overexpressing *aidB* had a considerably reduced frequency of mutation upon exposure to different concentrations

of MNNG. The protein encoded by *aidB* had significant sequence homology with several mammalian acyl-coenzyme A (CoA) and isovaleryl-CoA dehydrogenases. No sequence homology was detected with *ada*, *alkA*, *alkB*, or any other DNA repair proteins. Assays revealed that cell extracts overexpressing *aidB* demonstrated some isovaleryl-CoA dehydrogenase activity, although no values were reported. Also, no activity with other acyl-CoA's was observed.

Great emphasis has been placed on the transcriptional regulation of *aidB* by ^mAda and its interaction with different subunits of RNA polymerase. As mentioned above, when bound to the *aidB* promoter ^mAda interacts with a negatively charged patch of σ^{70} subunit of the RNA polymerase; specifically, the interaction involves residues Glu-574, Glu-575, Glu-591, Glu-605, and Asp-612 (34). More recent reports have shown that both the σ^S and σ^{70} forms of RNA polymerase can initiate transcription from the *aidB* promoter. However, it was observed that a functional *rpoS* gene is necessary for optimal ^mAda dependent *aidB* expression (66). It was also observed that σ^S could initiate transcription at the *aidB* promoter more efficiently than σ^{70} , both in the presence and absence of Ada (29-31).

Given the available information, the cellular function of AidB remains unclear. The AidB sequence reveals a close relationship to acyl-CoA dehydrogenases and crude cell extracts overproducing the protein exhibit isovaleryl-CoA dehydrogenase activity (33), but there is no obvious requirement for expression of another acyl-CoA dehydrogenase when cells are exposed to alkylating agents. Overexpression of *aidB* leads to reduced levels of mutagenesis caused by MNNG exposure (33), but the mechanism of protection against mutation is unknown. Although many questions about its function

remain, AidB has been hypothesized to repair unidentified DNA lesions or to detoxify certain S_N1 reagents (33, 35).

Focus of this Thesis.

As a first step to defining its role, I purified AidB and characterized several of its biophysical properties (Chapter 2). Specifically, I established that AidB is a flavin-containing protein with weak isovaleryl-CoA dehydrogenase activity. I describe features of a homology model of AidB constructed by Dr. William Wedemeyer based on the structure of a four-domain acyl-CoA oxidase, that reveals a positively charged groove connecting the active sites and a second canyon of positive charges. These features represent potential DNA-binding sites. Significantly, I demonstrated that AidB binds to dsDNA with a slight preference for the methylated polymer. Furthermore, I showed that binding to DNA protects a large region of AidB from proteolysis. I carried out additional studies (Chapter 3) that begin to address the physiological function of AidB by analysis of an *aidB* deletion strain. In addition, I provided protein to Dr. Allen Orville, a crystallographer, who has succeeded in generating AidB crystals. These studies set the stage for future efforts to characterize the function of AidB.

CHAPTER 2

CHARACTERIZATION OF THE Aid B COMPONENT OF THE *E. coli* ADAPTIVE RESPONSE TO METHYLATING AGENTS.

(A modified version of this chapter has been accepted for publication in the Journal of Bacteriology with the title “*The AidB Component of the Escherichia coli Adaptive Response to Alkylating Agents is a Flavin-Containing, DNA-Binding Protein*” with coauthors listed as Mukta S. Rohankhedkar, Scott B. Mulrooney, William J. Wedemeyer and Robert P. Hausinger. Dr. Mulrooney assisted me with the cloning and spectroscopy studies. Dr. Wedemeyer carried out sequence homology alignments and created the sequence homology model.)

Two general classes of environmental and laboratory chemicals are known to alkylate DNA. S_N1 reagents (e.g., methylnitrosourea and *N*-methyl-*N'*-nitro-*N*-nitrosoguanidine, MNNG) react primarily with the N^7 and O^6 positions of guanine, N^3 of adenine, O^6 or O^4 of pyrimidines, and the non-phosphodiester oxygen atoms of the phosphate backbone. In contrast, S_N2 agents (e.g., methylmethanesulfonate and dimethylsulfate) react primarily with the N^1 position of adenine and N^3 of cytosine (57). Microorganisms generate endogenous methylation compounds, such as *S*-adenosylmethionine, and are exposed to exogenous methylating substances that can modify their DNA, RNA, and other cellular components.

To overcome the mutagenic and toxic effects of DNA methylation, *Escherichia coli* possesses a variety of DNA repair enzymes, some of which are induced as part of the “adaptive response to alkylating agents” (57, 63, 64, 67, 68). A key component of this process is the Ada protein, associated with three distinct activities. The amino terminal domain of Ada catalyzes a methyl phosphotriester methyltransferase reaction that repairs methyl phosphotriesters in the DNA backbone while irreversibly methylating its Cys-38 side chain. Similarly, the carboxyl terminal domain of Ada possesses 4-meT and 6-meG methyltransferase activities that irreversibly methylate Cys-321. In addition to the single-turnover reactions catalyzed by Ada, the protein (in its Cys-38 methylated form) functions as an activator that enhances transcription of its own gene as well as those encoding AlkA, AlkB, and AidB. AlkA is a 3-meA DNA glycosylase that removes the alkylated base to create abasic sites in the DNA product. AlkB is an Fe(II)- and α -ketoglutarate-dependent hydroxylase that uses oxidative demethylation chemistry to reverse methylation damage to 1-meA and 3-meC (61). In contrast to the situation for

Ada, AlkA, and AlkB, the role of AidB in the adaptive response process remains uncharacterized.

The AidB sequence reveals a close relationship to acyl-coenzyme A (CoA) dehydrogenases, and crude cell extracts overproducing the protein exhibit isovaleryl-CoA dehydrogenase activity (33). Overexpression of *aidB* leads to reduced levels of mutagenesis caused by MNNG exposure (33), but the mechanism of protection against mutation is unknown. Curiously, some derivative strains with the gene insertionally inactivated exhibit enhanced tolerance to a methylating agent (67). This surprising result might be due to enhanced activity or stabilization of the protein in these constructs where the sites of insertion are localized to the 3' region of the gene. While many questions about its function remain, AidB has been hypothesized to repair unidentified DNA lesions or to detoxify certain S_N1 reagents (33, 35).

As a first step to defining its role, I purified AidB and characterized several of its biophysical properties. I established that AidB is a flavin-containing protein with weak isovaleryl-CoA dehydrogenase activity. A homology model of AidB, generated by Dr. William Wedemeyer and based on the structure of a four-domain acyl-CoA oxidase, revealed a positively charged groove connecting the active sites and a second canyon of positive charges. These features represent potential DNA-binding sites. Significantly, I demonstrated that AidB binds to dsDNA with a slight preference for the methylated polymer. Furthermore, the binding of DNA was shown to protect a large region of AidB from proteolysis. These studies set the stage for future efforts to characterize the function of AidB.

Materials and Methods

Images in this thesis are presented in color.

Cloning and expression of aidB.

The *aidB* gene of *E. coli* K12 (33) was amplified from host DNA by using the forward and reverse primers *aidB-Nco-F* 5'-AGG ATA TAC CAT GGA GGG AGA CAC AGT GCA C-3' (introducing an *NcoI* site at the 5'-end of the gene; start codon underlined) and *aidB-Hind-R* 5'-TCT CGT AGA AGC TTT TAC ACA CAC ACT CCC CCC G-3' (which introduces a *HindIII* site at the 3'-end of the gene). The amplified gene was digested with *NcoI* and *HindIII*, and subcloned into the *NcoI* and *HindIII* sites of a pET28a vector (Novagen) to create pET28aAidB. This plasmid was transformed into *E. coli* C41[DE3] (45) that was grown on LB agar plates containing kanamycin (50 µg/mL), and the construct was confirmed to be correct by analyzing the *NcoI* and *HindIII* digestion products on a 1% agarose gel and by DNA sequencing. Cultures were grown overnight at 37 °C with constant shaking at 200 r.p.m., and 1 mL was used to inoculate 1 L of TB medium (Fisher Biotech) containing kanamycin (50 µg/mL). Cells were grown at 37 °C to an OD₆₀₀ of ~0.4 following which IPTG was added (final concentration of 2 mM) and the cultures were allowed to grow overnight. Cells were harvested by centrifugation, resuspended in 30 mL lysis buffer (10 mM Tris, pH 7.8, containing 1 mM EDTA, 0.3 M NaCl, 20 % glycerol, 2 mM Tris(2-carboxyethyl)phosphine hydrochloride (TCEP; Pierce Biotechnology, Rockford, IL) as reductant, and 0.5 mM phenylmethylsulfonyl fluoride to prevent proteolysis), disrupted by sonication, and centrifuged at 27,000 x g for 2 h at 4 °C.

Purification of AidB.

The cell extracts were treated by using stepwise increasing concentrations of ammonium sulfate at room temperature, with each addition followed by centrifugation at 6,000 x g at 4 °C to pellet the precipitated protein. The pellet resulting from the 30-45 % ammonium sulfate treatment was dissolved in buffer A (10 mM Tris, pH 7.8, 1 mM EDTA, 20 % glycerol, 2 mM TCEP) containing 1 M NaCl, and the soluble proteins were applied to a phenylagarose column (Sigma, St. Louis, MO) equilibrated in the same buffer. Contaminating proteins were eluted by washing the column with buffer A lacking NaCl, and AidB was eluted with buffer A containing 0.4 % (w/v) deoxycholate. Fractions were analyzed by sodium dodecylsulfate polyacrylamide gel electrophoresis (SDS-PAGE) using a 10 % running gel (32). The fractions containing the protein of interest were pooled, applied to a DEAE Sepharose column equilibrated in buffer A, and eluted with a linear gradient from buffer A to 1 M NaCl in buffer A containing 0.02 % Triton-X100. Fractions were analyzed by 10% SDS-PAGE.

Native molecular weight of AidB

Size exclusion chromatography was performed by using a Protein-Pak™ 300SW (diol(OH) 10 µm, 7.5 mm x 300 mm) column equilibrated in buffer containing 10 mM Tris, pH 7.8, 0.3 M NaCl, and 10 % glycerol at 1 mL/min. The molecular weight of the native protein was estimated by comparing its retention time (monitored at 214 or 280 nm) to those of molecular weight standards (thyroglobulin, 670,000 Da; bovine γ-globulin, 158,000 Da; chicken ovalbumin, 44,000 Da; equine myoglobin, 17,000 Da; vitamin B₁₂, 1,350; Bio-Rad).

Characterization of the AidB cofactor.

Spectrophotometric quantification of the chromophore in AidB was carried out after denaturing the protein in 1% SDS. For cofactor identification, the intact AidB protein was applied to a matrix containing 2,5-dihydroxybenzoic acid and matrix-assisted laser desorption/ionization (MALDI)-mass spectrometric (MS) analysis was performed by using the Applied Biosystems Voyager System 4148. The observed m/z ratio was compared to that for an authentic standard of flavin adenine dinucleotide (FAD) (14).

The effects of chemical reduction on the UV-visible spectra of free and protein-bound FAD cofactor (26.41 μM) were assessed by titrating samples (purged with argon gas) with dithionite in an anaerobic cuvette while monitoring the absorbance (300 nm to 600 nm) with a Beckman DU 7500 or Hewlett-Packard HP8453 spectrophotometer. The concentration of dithionite used in this assay was quantified by monitoring the absorbance changes during analogous titration of protein-free FAD. Photoreduction of the flavin of AidB (4 μM subunit) was carried out by exposing an anaerobic sample (in buffer A containing 15 mM EDTA, 0.3 M NaCl, and 0.185 μM 5-deazaflavin; the latter was generously provided by Dave Arscott, Sumita Chakraborty, and Vincent Massey) to a 100 W halogen light (Philips narrow spot) source at a distance of 8.5 cm and at 0 °C. The absorbance spectrum (300 nm to 600 nm) was monitored every 5 min by using a Beckman DU 7500 spectrophotometer. Fluorescence spectra were acquired using a Perkin Elmer Luminescence spectrometer (model LS-50B).

Changes to the absorbance spectra of oxidized and fully-reduced AidB protein were examined in the presence of 1 mM CoA, 1 mM butyryl-CoA, 1 mM isovaleryl-CoA, or 100 mM MNNG. In addition, the absorbance spectrum of oxidized protein was

monitored upon addition of 5 mM sodium sulfite, 100 μ M NADH, 15 mM nitroethane, 200 μ M 5-meC, 200 μ M 7-meG, or 200 μ M 5-methyl-2-deoxycytidine. Finally, the effect on AidB cofactor fluorescence was examined for protein in the presence of 10 μ g/mL of a randomly chosen 29-mer of dsDNA.

Isovaleryl-CoA dehydrogenase activity assay.

Isovaleryl-CoA dehydrogenase activity assays were performed essentially as described previously (11), but omitting the phenazine methosulfate mediator and reductant. Assays were carried out at room temperature in 200 mM phosphate buffer, pH 8.0, and using purified recombinant protein that had been dialyzed to remove TCEP. Isovaleryl-CoA was synthesized as previously described (52) or purchased (Sigma). For routine assays, 2 mM isovaleryl-CoA was used as the substrate and 0.1 mM 2,6-dichlorophenolindophenol (DCPIP) was used as the terminal electron acceptor in a final volume of 300 μ l. The change in absorbance at 600 nm was monitored by using a Beckman DU 7500 spectrophotometer, and the enzyme activity was calculated by assuming an extinction coefficient of 20.6 mM⁻¹ cm⁻¹ for DCPIP (11).

DNA binding assays.

The ability of AidB to bind to DNA was assessed by three independent approaches. As one method, AidB (5 to 450 μ g) was applied to columns of dsDNA-cellulose (Sigma; 200 μ g calf thymus DNA per mL of resin; 1.0 X 10 cm) equilibrated in buffer A (except that TCEP was replaced by dithiothreitol), pH 8.0, and the columns

were washed in a stepwise manner with buffer solutions containing 0, 0.1, 0.5, and 1.0 M NaCl (8). Fractions eluting from the column were examined for AidB by SDS-PAGE.

A second technique to assess DNA binding by AidB focused on the ability of bound DNA to protect AidB from proteolysis. Linearized pCAT DNA (Novagen) (200 ng) was incubated with 50 μ g of purified AidB in 20 μ L buffer (20 mM Tris, 1 mM EDTA, pH 7.8) for 1 hr at 37 °C, chymotrypsin (Sigma) was added (1:20 w/w, protease:AidB), samples were incubated at 37 °C for 0, 3, or 6 h, and the reactions quenched by adding 0.3 volumes of 8 % trichloroacetic acid followed by incubation on ice. The extent of proteolysis and sizes of the resulting AidB fragments were identified by SDS-PAGE using gels comprised of 18 % polyacrylamide. The proteolytically-derived peptides were electroblotted (50 V for 3 hr at 4 °C) onto a polyvinylidene difluoride membrane using transfer buffer containing 10% methanol and 10 mM CAPS, pH 11 (43). After staining with 0.1% Coomassie R-250 in 40% methanol for 45 sec to identify the location of the desired band, the membrane was destained with several changes of 50% methanol and rinsed with water. The amino-terminal sequence of the desired AidB fragment was obtained at the MSU Macromolecular Structure, Sequencing, and Synthesis Facility by using an Applied Biosystems Procise cLC 494 Protein/Peptide Sequencer.

As a third approach, aliquots of pUC19 DNA (200 ng, Novagen) were incubated with AidB (1 μ M to 50 μ M) in 10 μ L buffer A at 37 °C for 30 min before being electrophoresed in a 1 % agarose gel using 40 mM Tris, pH 7.8, 1 mM EDTA buffer, as previously described (21). To probe the ability of AidB to bind to methylated DNA, pUC19 DNA was methylated by incubating it with 10 mM MNNG at 30 °C for 1 h. The

methyated plasmid DNA was purified by using spin columns (Qiagen) to remove excess MNNG and examined for interaction with AidB as described above. In some cases, the plasmid was treated with restriction enzymes prior to incubation with AidB.

Sequence analysis and homology modeling.

The full-length sequence of AidB was submitted to the Bioinfo.pl Meta Server (<http://bioinfo.pl/Meta/>) hosted by the BioinfoBank Institute of Poland (13). Secondary-structure predictions were carried out by using the four best-validated (26) secondary-structure servers, PsiPRED (22, 44), SABLE2 (2), SAM-T2K (23), and PROFsec (55). The results were parsed, formatted, and visualized using lab-written software that is publicly available as a web-server (http://proteins.msu.edu/Servers/Secondary_Structure/visualize_secondary_structure_prediction.html) and covered by the GNU General Public License.

PIR (protein information resource) alignments of full-length AidB to two parent structures, rat short chain acyl-CoA dehydrogenase (PDB accession code 1JQI) and rat liver peroxisomal acyl-CoA oxidase-II (PDB accession code 1IS2), were obtained from the PSI-BLAST (3) and FFAS03 (18) servers, respectively. These PIR alignments and the corresponding PDB files were converted into a homology model of AidB by using lab written software that is publicly available as a web-serve (http://proteins.msu.edu/Servers/Homology_Modeling/construct_homolog_PDB.html) and covered by the GNU General Public License. Ribbon illustrations of the models were generated by using MOLMOL (27) and electrostatic potential analyses utilized GRASP (50).

RESULTS

Purification of AidB

E. coli aidB was amplified by PCR to yield the expected 1.7 kb fragment which was cloned into the *NcoI-HindIII* site of pET28a (Novagen) and transformed into *E. coli* C41[DE3] cells. Using TB medium, optimal production of AidB was observed following overnight growth at 37 °C and using 2 mM IPTG (data not shown). Following sonication and centrifugation, cell extracts were treated with increasing concentrations of ammonium sulfate, and the desired protein was found to precipitate in the 30 % - 45 % fraction. The resolubilized sample was subjected to phenyl Sepharose chromatography, with elution requiring low salt and inclusion of 0.4% (w/v) deoxycholate, to provide yellow fractions that contained a protein coinciding with the predicted molecular weight of 60,900 Da (Figure 2.1). The pooled sample was purified to apparent homogeneity by DEAE-Sepharose chromatography in buffer that contained 0.02 % Triton-X100 to enhance the protein stability. The typical yield was 30 mg of protein per L of culture. Purified protein was stored in this buffer at 4 °C.

Biophysical characterization of AidB

On the basis of its retention time during size exclusion chromatography and comparison to standard proteins, AidB was estimated to possess a molecular weight of $200,000 \pm 30,000$ Da (data not shown). Given that the monomer molecular weight is predicted to be 60,090 Da, the sample is most consistent with a homotrimeric or homotetrameric quaternary structure.

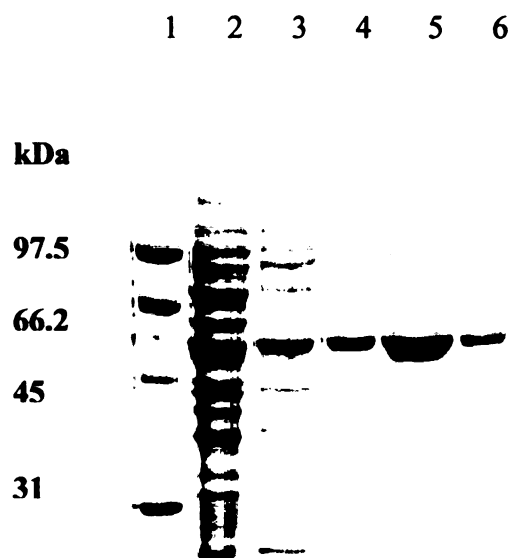


Figure. 2.1: SDS-PAGE analysis of AidB purification. AidB was isolated from extracts of *E. coli* C41 [DE3] cells containing pET28aAidB by ammonium sulfate precipitation followed by successive chromatography using phenyl-Sepharose and DEAE-Sepharose columns. Fractions were analyzed by using 10 % SDS PAGE. Lane 1, standards; lane 2, cell extracts; lane 3, 30 – 45 % ammonium sulfate pellet dissolved in buffer A; lanes 4 and 5, Phenyl-Sepharose fractions; lane 6, DEAE-Sepharose pooled fractions.

AidB was examined for the presence of a flavin cofactor, suspected from the protein's distinctive yellow color and the known sequence homology to acyl-CoA dehydrogenases and oxidases. The absorbance spectrum of purified AidB exhibited major features at 460 and 370 nm, consistent with the presence of a flavin. On the basis of the absorbance intensity at 460 nm and an FAD ϵ_{450} of 11,300 M⁻¹cm⁻¹, AidB was estimated to contain 0.92 moles of flavin per mole of subunit. Direct confirmation of the presence of FAD (as opposed to FMN or riboflavin) was obtained by MALDI-MS analysis that revealed a feature at m/z of 787.60 (data not shown), agreeing well with the calculated value of 785.16 for FAD (14). The FAD cofactor bound to AidB was examined for its fluorescence properties by scanning excitation wavelengths from 300 to 500 nm and measuring emission at 520 nm. No significant emission was detected, indicating that the fluorescence of the FAD is highly quenched when bound to the protein.

To further characterize the AidB-bound flavin, the protein was treated with the chemical reducing agent sodium dithionite in an anaerobic cuvette. As illustrated in Figure 2.1, titration of the enzyme (26.4 μ M subunit) with a solution of dithionite led to changes in the absorbance spectra that were consistent with three distinct phases. The first few additions of reductant did not affect the absorbance, presumably because residual oxygen was being consumed. Further addition of up to one equivalent of dithionite resulted in a steady decrease in absorbance at 450 nm and an increase in absorbance at 372 nm. Continued addition of dithionite resulted in a uniform decrease in absorbance across the spectrum, ending with the completely reduced form of protein-bound FAD. In contrast, titration of protein-free FAD with dithionite (used to quantify the concentration of the dithionite reductant) led to a monotonic conversion of the

oxidized to the reduced flavin (spectra not shown). The intermediate observed during reduction of the protein corresponds to the stable, one-electron reduced anionic semiquinone; formation of this stable species is characteristic of many flavoprotein oxidases (38). Unlike most flavin-containing oxidases (40), however, the protein did not react with added sulfite as shown by the lack of any spectroscopic change.

In the presence of EDTA, free flavins are known to efficiently catalyze the photo-reduction of a wide variety of flavoproteins (39, 41); thus, additional AidB flavin reduction studies were carried out using 5-deazaflavin and excess EDTA in the presence of light. Photoreduction of AidB for 30 min converted the enzyme-bound FAD to the anionic semiquinone state, but no additional changes were observed upon further incubation (Figure 2.3). These observations provide added support that the one-electron reduced form of the enzyme is stable, perhaps due to the presence of a positively charged side chain near the anionic N¹ of the flavin. The enzyme-bound flavin in both the semiquinone and fully reduced states was reoxidized upon incubation in the presence of oxygen.

Several other additives were examined for their effects on the AidB flavin spectrum. No perturbation of the visible spectrum was observed upon addition of NADH, sulfite (see above), CoA, butyryl-CoA, or isovaleryl-CoA to the oxidized enzyme. Similarly, neither the methylating agent MNNG nor nitroethane (a substrate for the flavoenzyme nitroalkane oxidase (47)) led to any changes in the FAD spectrum. CoA, butyryl-CoA, isovaleryl-CoA, and MNNG also failed to affect the spectrum of fully reduced enzyme (data not shown).

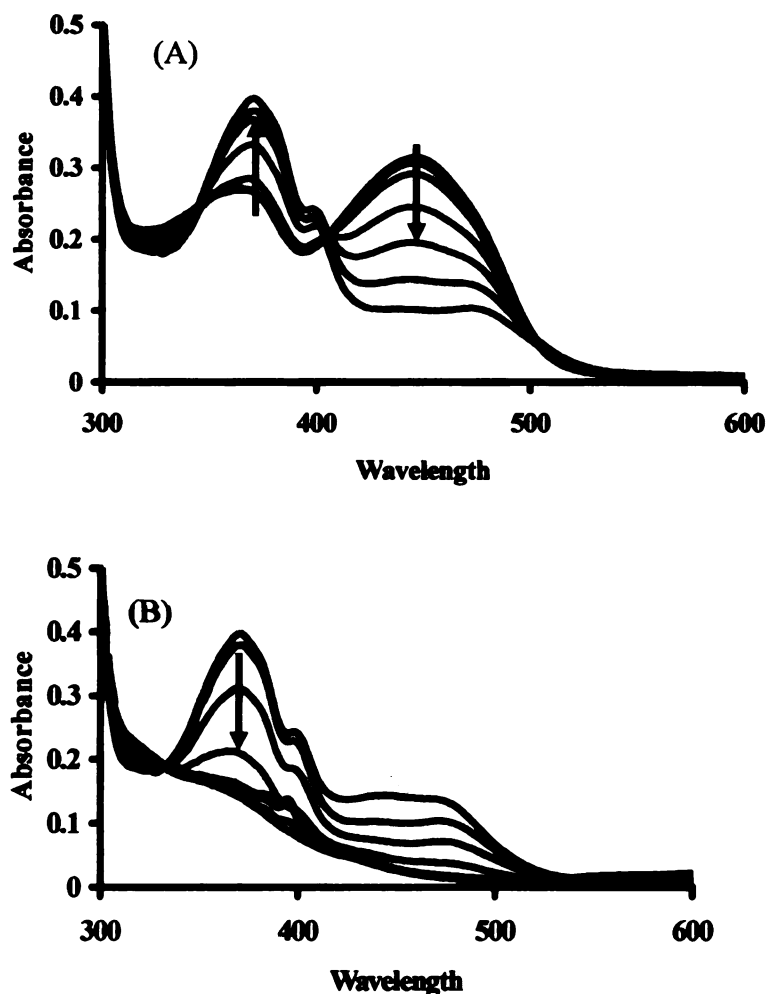


Figure 2.2: Dithionite titration of AidB. The changes in the spectrum of AidB (26.4 μ M protomer) in 1 ml of buffer containing 1X T.E with 0.02 % tritonX-100, 20 % glycerol and 2 mM DTT, pH 7.8, were monitored anaerobically during addition of 2 μ l aliquots of dithionite (1.028 mM stock). The concentration of the dithionite solution was determined by anaerobic titration of a stock FAD solution. (A) The initial traces at first exhibited little change, followed by reduction of the enzyme to the one-electron reduced anionic state that is characterized by the intense absorbance feature at 375 nm. (B) Subsequent reduction generated the two-electron reduced state.

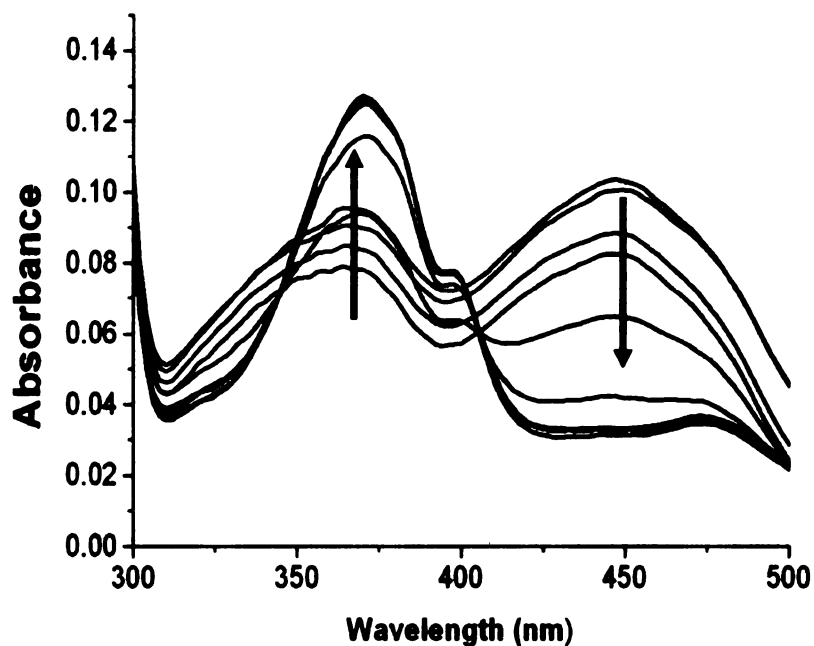


Figure 2.3: Photoreduction of AidB. An anaerobic sample of AidB ($\sim 4 \mu\text{M}$ subunit concentration) was photoreduced in the presence of excess EDTA and deaza FAD by using a 50 W halogen lamp while monitoring changes in its spectrum at 5 min intervals. The final AidB spectrum corresponds to the one electron reduced flavin state.

Enzymatic characterization of AidB.

Using the artificial electron acceptor DCPIP, AidB was confirmed to possess low levels of isovaleryl-CoA dehydrogenase activity ($0.0060 \pm 0.0022 \mu\text{moles min}^{-1} (\text{mg protein})^{-1}$ when using 2 mM acyl-CoA substrate). The presence of DNA did not influence the level of dehydrogenase activity significantly.

DNA binding by AidB.

AidB was suspected to bind to DNA on the basis of its co-regulation with DNA-repair enzymes and because a short region of its C-terminus was homologous to a DNA-binding region of topoisomerase I (see next section). To further test this hypothesis, three approaches were used to evaluate whether AidB binds DNA. First, AidB was shown to be retained by a column of dsDNA-cellulose, but could be eluted with 0.5 M NaCl (Figure 2.4). Second, the presence of dsDNA was shown to protect a domain of AidB (~50 kDa) from digestion by chymotrypsin (Figure 2.5). N-terminal sequencing of the protected fragment revealed an amino acid sequence of SNTTRAERLE, consistent with cleavage after residue Met-194 (predicted to be located in a flexible loop of the protein, see below) to produce a C-terminal fragment with the predicted size of 50,257 Da. Finally, gel band mobility shift studies demonstrated that AidB binds to dsDNA (Figure 2.6). Remarkably, dsDNA:AidB interaction resulted in a shift of the dsDNA band to the top of the gel as if each protein molecule is capable of binding to multiple molecules of dsDNA and each DNA molecule binds several AidB proteins, resulting in aggregation. DNA retardation was not observed when using heat denatured (~70 °C for 5 min) AidB

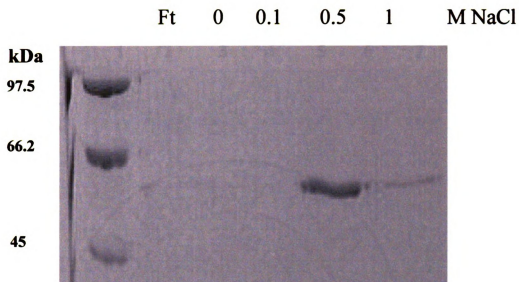


Figure 2.4: Binding of AidB to DNA cellulose. 200 $\mu\text{g/ml}$ of calf thymus DNA cellulose was packed in a 1 X 10 cm column in a buffer containing 1X TE, 20 % glycerol and 2 mM DTT. 5-450 μg of purified AidB was incubated with the DNA cellulose and then eluted in a step wise manner with the above mentioned buffer supplemented with 0.1, 0.5 and 1 M NaCl. All fractions were collected separately and analyzed by 10 % SDS PAGE.

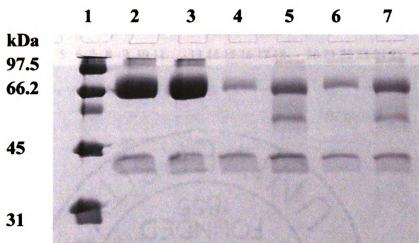


Figure 2.5: DNA-induced protection against protease digestion of an AidB domain.

AidB (50 μ g) was digested with 2.5 μ g of chymotrypsin for 0, 3, or 6 hr in the absence of DNA (lanes 2, 4, and 6) or in the presence of 200 ng of plasmid DNA (lanes 3, 5, and 7) at 37 °C. The reactions were quenched with trichloroacetic acid and the samples analyzed by SDS-PAGE on an 18 % gel. Lane 1 contains molecular weight markers (97.4, 66.2, 45, 31, 21.5, and 14.4 kDa). The band located above the 31-kDa marker and found in lanes 2-7 is chymotrypsin.

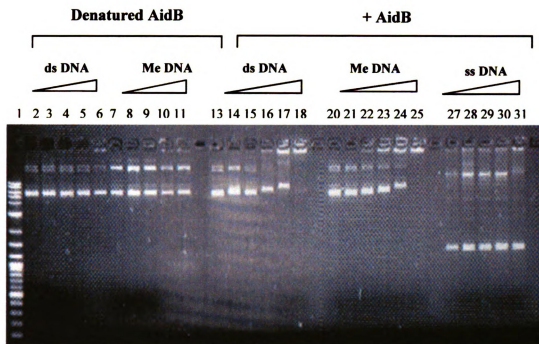


Figure 2.6: AidB-induced mobility shift of dsDNA. Varied concentrations (0 μM , 0.1 μM , 0.5 μM , 0.75 μM , 1 μM and 2 μM) of heat-denatured AidB (lanes 2-11) or native AidB (lanes 13-31) were incubated with non-methylated dsDNA (lanes 2-6 and 13-18), methylated dsDNA (lanes 7-11 and 20-25), and ssDNA (lanes 27-31) for 1 hr at 37 $^{\circ}\text{C}$ prior to analysis on a 1 % agarose gel. The DNA samples included 200 ng pUC19 dsDNA or M13 phage ssDNA in 10 μl of buffer (pH 7.2). AidB was denatured by heating it to ~ 70 $^{\circ}\text{C}$ for 5 min prior to incubation with DNA. Lane 1 shows the New England Biolabs 2-log DNA ladder as the standard.

(lanes 2-11), and little interaction was noted when using ssDNA (lanes 27-31). Of potential functional significance, repeated experiments demonstrated that slightly lower concentrations of AidB were required to perturb the migration of MNNG-treated DNA (lanes 20-25) compared to non-methylated sample (lanes 13-18). Consistent with the absence of precise DNA sequence specificity, AidB was shown to shift each of the bands arising from *EcoRI* digestion of pCAT plasmid DNA and to bind to a randomly selected 29-mer dsDNA oligomer (data not shown). In addition, methylated 29-mer dsDNA was bound more tightly than the non-methylated oligomer according to mobility shifts in a 4 – 20 % gradient polyacrylamide gel.

Sequence analysis and homology modeling.

Preliminary analysis using the bioinfo.pl server showed that the *N*-terminal 440 residues of the 541-residue AidB are homologous to the acyl-CoA dehydrogenases (12), a family of enzymes that form tightly bound homodimers or homotetramers and typically have three domains: an *N*-terminal α -helical domain, a middle β -sheet domain, and a *C*-terminal helical bundle (25). The dimeric structure of a related protein family member, rat liver peroxisomal acyl-CoA oxidase II (PDB accession code 1IS2), features a fourth helical domain (48). A consensus of secondary-structure servers agreed that the *C*-terminal 102 residues of AidB are α -helical and consistent with the 1IS2 structure (Data not shown). Therefore, we made a homology model of the full-length AidB homodimer using 1IS2 as the parent structure (Figure 2.7). This four-domain model is best

understood after carrying out a detailed sequence comparison of AidB analogues to identify critical residues, as described below.

To identify full-length homologues of AidB (versus the many acyl-CoA dehydrogenases resembling only the three *N*-terminal domains), its *C*-terminal 102 amino acid residues were submitted to the NCBI PsiBLAST server (<http://www.ncbi.nlm.nih.gov/BLAST>). After seven rounds of PsiBLAST, no new homologues were identified above the $E = 0.005$ level. In all, PsiBLAST identified 57 homologues of AidB of similar lengths, 550 ± 13 residues (2σ deviation). These sequences, all annotated as putative acyl-CoA dehydrogenases, were filtered to remove sequences with greater than 90% identity, producing a non-redundant set of 34 homologous sequences. The closest hits were from two related enterobacteria, *Salmonella* and *Yersinia*, but hits were also identified from some γ -Proteobacteria (*Pseudomonas*, *Idiomarina*, *Azotobacter* and *Acinetobacter*), β -Proteobacteria (*Burkholderia*, *Ralstonia*, *Chromobacterium*, *Azoarcus* and *Bordetella*), α -Proteobacteria (*Brucella*, *Bartonella*, *Rhodopseudomonas*, and various *Rhizobia*) and even Gram-positive bacteria (*Mycobacterium*, *Streptomyces*, *Nocardia* and *Desulfitobacterium*).

The 34 non-redundant, full-length AidB-like sequences were aligned (data not shown) using the T-Coffee webserver (<http://igs-server.cnrs-mrs.fr/Tcoffee/tcoffee.cgi/index.cgi>), which is the best-validated multiple sequence alignment method (26). Despite the evolutionary distance between the organisms, AidB is highly conserved, with no less than 67 absolutely conserved residues (numbering based on the *E. coli* AidB sequence):

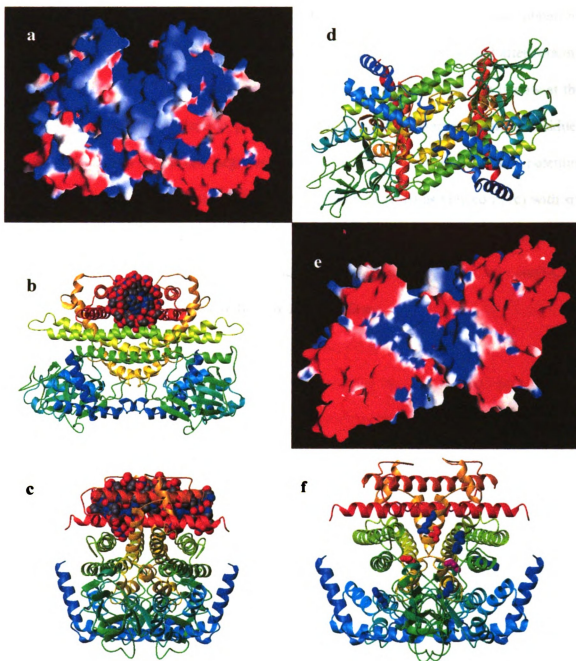


Figure 2.7: Homology model of AidB. (a) An electrostatic potential analysis of the homodimer, with positive charge in blue and negative charge in red, depicting a positively charged canyon created by the C-terminal region of the protein. (b) The same view shown as a ribbon diagram, with the chain color varying from blue to red progressing from the N- to C-terminus, with a dodecamer of B-form DNA manually

positioned in the positively charged canyon at the top. (c) The same molecule rotated by 90 ° around a vertical axis. (d) Ribbon diagram of the homodimer as viewed after rotating the structure in (a) and (b) by ~ 90 ° around a horizontal axis. The canyon is now at the back of the molecule. A shallow groove is depicted with conserved positive residues shown in blue and conserved negative residues in red. (e) An electrostatic potential analysis of AidB in the same view. (f) Ribbon diagram of AidB as viewed in (c) with six conserved positively charged residues, three conserved negatively charged residues, and a conserved Cys, all located at the substrate-binding site of acyl-CoA dehydrogenases/oxidases, shown in blue, red, and yellow.

Asn10, Ala62, Pro67, Gly76, Arg78, Pro86, Cys133, Pro134, Met137, Thr138,
Lys175, Gly181, Thr185, Glu186, Lys187, Gln188, Gly189, Gly190, Asp192, Ala200,
Gly212, His213, Lys214, Phe216, Ser218, Pro220, Asp223, Cys237, Phe238, Pro241,
Asn250, Leu257, Lys258, Lys260, Gly262, Asn263, Asn266, Ser268, Glu270, Glu272,
Gly282, Gly287, Met294, Thr298, Arg299, Arg311, Arg324, Leu331, Met337,
Arg375, Lys382, Glu395, Glu398, Gly401, Gly402, Gly404, Arg413, Glu417, Pro419,
Trp424, Glu425, Gly426, Gly428, Asn429, Asp434, Arg437, and Arg483. The residues
 shown in bold are identical in AidB-like sequences, but not highly conserved among the
 non-AidB-like homologues; non-bold residues are nearly universally found, or
 conservatively replaced, in the entire group of acyl-CoA dehydrogenases. In addition,
 five charges are conserved absolutely: **Glu128, Asp166, Arg242, Glu407 and Arg416,**
 again with bold indicating that all five are conserved in the AidB-like homologues, but
 not in non-AidB-like acyl-CoA dehydrogenases. The absolutely conserved residue
 Glu425 corresponds to the catalytic glutamate in most of the short- and medium-chain
 acyl-CoA dehydrogenases. Of interest, this residue is an alanine in human isovaleryl-
 CoA dehydrogenase that uses Glu254 as the general base, whereas AidB **Thr298,**
 absolutely conserved in AidB-like sequences, corresponds to the catalytic glutamate
 found in the long-chain acyl-CoA and isovaleryl-CoA dehydrogenases. The conservation
 of Glu425 suggests that a dehydrogenase or oxidase activity is essential to the
 physiological function of AidB.

The homodimer structure (Figure 2.7) has three noteworthy features that may
 pertain to the function of AidB. *First*, there is a prominent “canyon” composed mainly of
 the C-terminal helical hairpin stacked across similarly long helices of the third domain.

The canyon has a strong positive electrostatic potential (Figure 2.7a) and has the correct dimensions (~20 Å wide, ~20 Å deep, and ~40 Å long) to accommodate a 12 bp stretch of dsDNA, as illustrated by the models (Figure 2.7bc) that include a Dickerson-Drew dodecamer of B-form DNA (9). This domain also exhibits weak similarity (17 identities over 47 AidB residues) to a DNA-binding domain of human topoisomerase I, further supporting our hypothesis that dsDNA binds to this region of AidB. *Second*, the opposite face has a more shallow groove lined with conserved positive charges from both subunits, specifically, **Arg78**, **Lys187**, **His213**, **Lys258** and **Lys260** from one subunit and **Arg324**, **Arg413** and **Arg416** from the other (16 blue side chains of Figure 2.7d). Of these residues, only Arg324 is widely distributed in non-AidB-like acyl-CoA dehydrogenases. There is one conserved negative charge in the center of the groove (**Glu407**) and two (**Glu270**, **Glu272**) on its periphery (six red side chains in Figure 2.7d), with these residues not well conserved in non-AidB-like sequences. The electrostatic potential of this region is generally positive (Figure 2.7e), consistent with this symmetric groove being a secondary DNA binding site. This groove is oriented at approximately 45° relative to the putative DNA-binding canyon described above. *Third*, the catalytic substrate binding site also is lined with conserved positive charges (blue side chains in Figure 2.7f), namely, **Lys214**, **Arg242**, **Arg299**, **Arg375**, **Lys382**, and **Arg437** (all from the same subunit), three conserved negative charges (**Asp192**, **Asp434** and the catalytic **Glu425**, shown as red side chains in Figure 2.7f) and a conserved cysteine residue, **Cys237** (shown in yellow in Figure 2.7f). Only three of these residues (**Lys214**, **Lys382**, and **Glu425**) are conserved beyond the AidB-like sequences.

AidB can be aligned with acyl-CoA dehydrogenases that form homotetramers, such as isovaleryl-CoA dehydrogenase (25), from which a tetrameric model of AidB could be constructed. However, the tetramerization interface of these enzymes coincides with the predicted location of the C-terminal helices that we have suggested form a DNA-binding “canyon”. Therefore, we cannot reliably propose such a homotetramer model.

DISCUSSION

Characterization of AidB as a flavin-containing isovaleryl-CoA dehydrogenase.

The results described above present the first reported purification of AidB, a component of the *E. coli* adaptive response to alkylating agents. Consistent with expectations based on sequence comparisons and in agreement with the observed activity in crude cell extracts (33), purified AidB is a flavin-containing enzyme with isovaleryl-CoA dehydrogenase activity. Curiously, AidB possesses a Glu residue (position 425) at the position of the active site carboxylate base found in most acyl-CoA dehydrogenases, whereas human isovaleryl-CoA dehydrogenase possesses an Ala at this position and utilizes a Glu on a distinct helix as its general base (25). The level of isovaleryl-CoA dehydrogenase activity observed in AidB is quite low when compared to other acyl-CoA dehydrogenases. For comparison, human isovaleryl-CoA dehydrogenase exhibits 8.2 to 11.7 $\mu\text{moles min}^{-1} (\text{mg protein})^{-1}$ under similar conditions, or >1000-fold higher activity (5, 46). In addition, human butyryl-CoA dehydrogenase (10), human glutaryl-CoA dehydrogenase (37), and various rat acyl-CoA dehydrogenases (16) exhibit specific activities of 7.4 to 15.3 $\mu\text{mol min}^{-1} (\text{mg protein})^{-1}$ using this assay. I conclude that

isovaleryl-CoA dehydrogenase activity in AidB is a side reaction that is distinct from its functional role.

Identification of AidB as a DNA-binding protein.

I demonstrated that AidB binds to dsDNA-cellulose, is protected from proteolysis by added dsDNA, and causes a mobility shift of dsDNA bands in native gels. This interaction between AidB and dsDNA was quite surprising given the sequence homology of AidB to acyl-CoA dehydrogenases, but is compatible with AidB possessing a methylated dsDNA repair activity. The gel band shift assays indicate a slight, but experimentally reproducible, higher affinity for binding to methylated samples. No sequence specificity was observed when examining large plasmid fragments, but further studies are warranted to characterize this in greater detail.

Quaternary structure of AidB.

The gel-permeation chromatographic properties of AidB are consistent with a trimeric or tetrameric quaternary structure, but on the basis of its structural relationships to acyl-CoA dehydrogenases/oxidases (which are all found to be dimers or tetramers) (25), I conclude that AidB is most likely a tetramer. Thus, the homology model shown in Figure 2.7 represents only half of the native size of the molecule. A less likely alternative is that AidB forms a homodimer with unstructured regions that cause the protein to have an unusually large hydrodynamic volume for its mass.

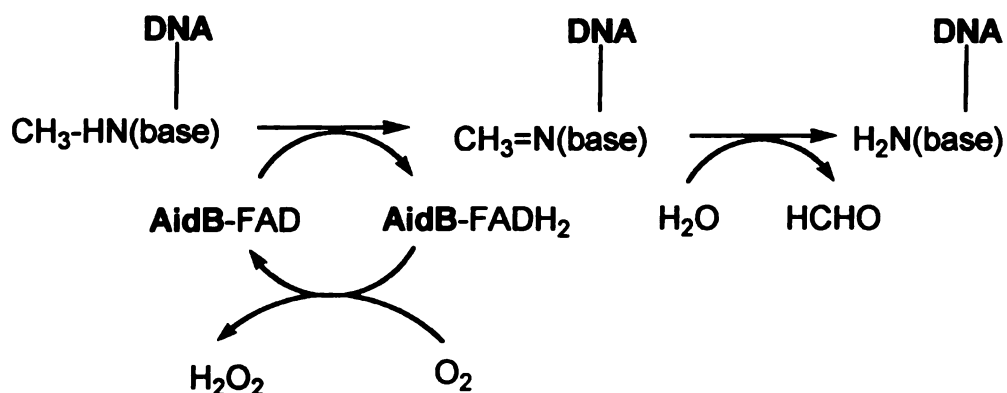
Predicted structure of AidB.

Overall, AidB seems likely to adopt a four-domain fold similar to rat liver peroxisomal acyl-CoA oxidase II (1IS2). A homology model of an AidB homodimer using this parent structure reveals a groove of positively charged residues that are absolutely conserved among full-length AidB homologues, but not among non-AidB-like acyl-CoA dehydrogenases. This groove connects the two putative active sites, which are themselves lined with absolutely conserved positive charges, a single cysteine (Cys237) and a glutamate that is necessary for catalysis in the structurally homologous short- and medium-chain acyl-CoA dehydrogenases. I propose that the groove binds ~20 bp of dsDNA, positioning it near the active sites. At least one acyl-CoA dehydrogenase family member binds to a large molecule substrate; i.e., FkbI functions in FK520 biosynthesis and binds acylated acyl carrier protein (69).

Interestingly, the fourth domain of AidB (residues 440-541) in the homology model forms a deep “canyon” that seems likely to bind double-stranded DNA. This domain is poorly conserved, however, and dsDNA bound in this canyon would have difficulty in reaching the putative active site, requiring a sharp turn that is inconsistent with the known stiffness of dsDNA. This is true even for models of tetrameric AidB in which dsDNA bound in the canyon of one dimer could in principle bind in the active site of the other homodimer. These features lead me to hypothesize that the fourth domain does not directly influence catalysis but serves a structural role; e.g., a “scaffolding” that binds to DNA, stabilizes the relative position of the subunits in the homodimer and, possibly, precisely positions the catalytic residues.

Potential cellular function of AidB.

Although AidB's role in the cell remains unknown, the presence of an enzymatically active flavin and the protein's demonstrated DNA-binding capability suggests that AidB uses a dehydrogenase activity to repair alkylated DNA by a mechanism such as that shown in Scheme. 2.1 (note that reoxidation of the reduced flavin is shown to occur by an oxygenase reaction, but electron donation to a separate electron carrier is another reasonable option). Several small molecules are known to be dealkylated by such oxidase mechanisms, including methylglycine (24), polyamines (36), and γ -*N*-methylaminobutyrate (7). In addition, precedent for demethylation of methylated proteins by the LSD1 flavoenzyme, a methylated histone demethylase, was recently reported to use this mechanism (58). Alternatively, a flavin-dependent monooxygenase activity could be invoked to repair alkylation damage. Further experiments to delineate the function of AidB are in progress. Interestingly, full-length AidB homologues are *not* detected in many bacteria closely related to *E. coli*, such as *Klebsiella*, *Vibrio*, *Shewanella* and *Photorhabdus* that possess other alkylation repair enzymes. The number of homologues of AidB seems to be far fewer than those of AlkA and AlkB. Whereas *ada* and *alkB* form a transcriptional unit, *alkA* and *aidB* are well-separated from this operon and from each other, raising the possibility that AidB may be of secondary importance for repair of alkylation damage to DNA.



Scheme 2.1: Hypothetical function of AidB. On the basis of its FAD cofactor and its ability to bind to methylated DNA, AidB might function as a methylated base dehydrogenase. The Schiff's base product would hydrolyze to release the free base plus formaldehyde, and the reduced flavin could either react with oxygen to produce hydrogen peroxide (as shown) or transfer electrons to another suitable electron acceptor. Analogous chemistry is possible for demethylation of bases alkylated at certain oxygen atoms.

CHAPTER 3

CONCLUSIONS AND FUTURE DIRECTIONS

The goal of this thesis was to characterize AidB, a protein that is part of the *E. coli* “adaptive response pathway” to DNA damage. This pathway includes the Ada protein that recognizes DNA damaged by methylating agents, transfers certain methyl groups onto itself, and serves as a specific transcription factor in its methylated form denoted ^mAda of four genes: *ada*, *alkA*, *alkB*, and *aidB*. While Ada, AlkA and AlkB had been well characterized and shown to catalyze DNA repair, the function of AidB remained a mystery. It had been reported that cells over expressing *aidB* showed increased tolerance to S_N1 type of methylating agents such as MNNG; however this activity had never been quantified and no studies had characterized the isolated protein.

The initial part of this study deals with the cloning and over-expression of *aidB*, the isolation of the encoded protein, and the characterization of its properties. I determined that AidB is a flavoprotein with weak isovaleryl-CoA dehydrogenase activity, in agreement with expectations from a similar activity reported in cell extracts. I showed that chemical reduction of the flavin moiety of AidB with sodium dithionite proceeds in two stages, with the flavin going through a stable anionic semiquinone before being completely reduced. I further showed that photoreduction of the flavin yields a stable one-electron reduced state. I used gel mobility shift assays to reveal that AidB binds to double stranded MNNG-methylated and unmethylated DNA, with a preference for the former. Using protease protection assays I showed that DNA binding protected a ~50-kDa domain of the 61-kDa protein from digestion. Finally, I compared the N-terminal 440 residues of the 541-residue AidB to the sequences of acyl-CoA dehydrogenases and analyzed a homology model (generated by Professor William Wedemeyer using 1IS2 as

the parent structure) of the full-length AidB homodimer. These efforts highlighted the AidB residues and domains that are potentially involved in DNA binding.

Although I've made good progress in characterizing many properties of AidB, the function of the protein in the cell remains unanswered. The very low levels of isovaleryl-CoA dehydrogenase that I detected with the purified protein indicate that it is a secondary activity of the protein. While previous reports have indicated that AidB could function as a DNA repair protein upon challenge with MNNG, further experiments need to be performed to substantiate this claim. I have recently obtained an *aidB* knockout strain (provided by Dr. Hirotada Mori at the Nara Institute of Science and Technology Research and Education Center for Genetic Information, Japan) and have initiated experiments to determine their survival upon MNNG treatment in comparison with the wild-type strain. I will examine the effects of using different inducing concentrations of MNNG on the survival rates of the knockout strain, the wild-type strain and the *aidB* overexpressing strain (6). These experiments should begin to provide valuable information about the physiological relevance of AidB in the *E. coli* cell and its potential role in protecting the cell against methylating agents. In order to determine the role of AidB in preventing damage induced mutagenesis, future studies by other investigators could include analysis of Ames strains. P1 mediated transduction from the present knock-out strain can be used to create an *aidB* deletion in the appropriate Ames strain. The deletion strain thus created, along with the wild type and an *aidB* overexpressing strain, could be treated with increasing concentrations of MNNG and assayed for the rate of reversion of amino acid auxotrophy. If AidB protects the *E. coli* cells from MNNG induced mutagenesis, then the *aidB* overexpressing strain should show the least number of revertants.

As mentioned above, sequence homology based modeling was used to develop a putative model of AidB. Even though AidB shows highest sequence homology to acyl-CoA dehydrogenases, it shows a very low specific activity with isovaleryl-CoA as the substrate. No activity was detected when other acyl-CoA's were used. To get a better understanding of the structure of the protein, attempts are being made, in collaboration with Dr. Allen Orville (Georgia Institute of Technology), to determine the crystal structure of AidB. Preliminary results have yielded small, needle-like crystals of AidB (Figure 3.1) using 30 % dioxane with 0.1 M MES, pH 5.5, at room temperature. Attempts are being made to grow larger crystals and to expand the set of conditions used to obtain them. If better crystals are obtained, they would yield valuable information about the structure of AidB and lend important clues regarding its physiological role.

Sequence homology-based analysis revealed that AidB has a 100 amino acid carboxyl terminal extension that is absent in other acyl-CoA dehydrogenases. Preliminary sequence homology analysis of this region showed that it has a low homology to the DNA binding helix of human topoisomerase I. Further analysis of this region by Dr. Wedemeyer revealed that the carboxyl terminal extension of AidB has 4 α -helical regions, similar to those seen in DNA topoisomerase I. In light of these similarities, it could be hypothesized that at least a portion of the DNA binding activity demonstrated by AidB could be attributed to this region. I have created a deletion mutant of this region and future efforts could include studies to overexpress and purify this truncated protein. Once this is accomplished, DNA binding studies could be carried out to test if the loss of the carboxyl terminal 100 amino acid residues affects the DNA binding ability of AidB.

These studies along with the information I have already collected should provide valuable information about the physiological role of AidB in the *E. coli* cell.



Figure 3.1: Crystals of AidB. Crystals of AidB were obtained at the Orville lab (Georgia Institute of Technology) using 30 % dioxane with 0.1 M MES, pH 5.5, at room temperature.

REFERENCES

1. **Aas, P. A., M. Otterlei, P. O. Falnes, C. B. Vagbe, F. Skorpen, M. Akbari, O. Sundheim, M. Bjoras, G. Slupphaug, E. Seeberg, and H. E. Krokan.** 2003. Human and bacterial oxidative demethylases repair alkylation damage in both RNA and DNA. *Nature* **421**:859-863.
2. **Adamczak, R., A. Porollo, and J. Meller.** 2005. Combining prediction of secondary structure and solvent accessibility in proteins. *Proteins: Struct. Funct. Genet.* **59**:467-475.
3. **Altschul, S. F., T. L. Madden, A. A. Schaffer, J. H. Zhang, Z. Zhang, W. Miller, and D. J. Lipman.** 1997. Gapped BLAST and PSI-BLAST: A new generation of protein database search programs. *Nucl. Acids Res.* **25**:3389-3402.
4. **Aravind, L., Walker, D.R., Koonin, E.V.** 1999. Conserved domains in DNA repair proteins and evolution of repair systems. *Nucl. Acids Res.* **27**:1223-1242.
5. **Battaile, K. P., M. McBurney, P. P. Van Veldhoven, and J. Vockley.** 1998. Human long chain, very long chain and medium chain acyl-CoA dehydrogenases are specific for the S-enantiomer of 2-methylpentadecanoyl-CoA. *Biochim. Biophys. Acta* **1390**:333-338.
6. **Calmann, M. A., Evans, J.E., Marinus, M.G.** 2005. MutS inhibits RecA-mediated strand transfer with methylated DNA substrates. *Nucl. Acids Res.* **33**:3591-3597.
7. **Chirabau, C. B., C. Sandu, M. Fraaije, E. Schiltz, and R. Brandsch.** 2004. A novel γ -N-methylaminobutyrate demethylating oxidase involved in catabolism of the tobacco alkaloid nicotine by *Arthrobacter nicotinovorans* pAO1. *Eur. J. Biochem.* **271**:4677-4684.
8. **deHaseth, P. L., C. A. Gross, R. R. Burgess, and M. T. Record, Jr.** 1977. Measurement of binding constants for protein-DNA interactions by DNA-cellulose chromatography. *Biochemistry* **16**:4777-4783.
9. **Drew, H. R., R. M. Wing, T. Takano, C. Broka, S. Tanaka, K. Itakura, and R. E. Dickerson.** 1981. Structure of a B-DNA dodecamer: conformation and dynamics. *Proc. Natl. Acad. Sci. USA* **78**:2179-2183.
10. **Eder, M., F. Krautle, Y. Dong, P. Vock, V. Kieweg, J. J. Kim, A. W. Strauss, and S. Ghisla.** 1997. Characterization of human and pig kidney long-chain-acyl-CoA dehydrogenases and their role in beta-oxidation. *Eur. J. Biochem.* **245**: 600-607.
11. **Engel, P. C.** 1981. Butyryl-CoA dehydrogenase from *Megasphaera elsdenii*. *Meth. Enzymol.* **71**:359-366.

12. **Ghisla, S., and C. Thorpe.** 2004. Acyl-CoA dehydrogenases. A mechanistic overview. *Eur. J. Biochem.* **271**:494-508.
13. **Ginalski, K., A. Elofsson, D. Fisher, and L. Rychlewski.** 2003. 3D-Jury: a simple approach to improve protein structure predictions. *Bioinformatics* **19**:1015-1018.
14. **Halada, P., C. Leitner, P. Sedmera, D. Haltrich, and J. Volc.** 2003. Identification of the covalent flavin adenine dinucleotide-binding region in pyranose 2-oxidase from *Trametes multicolor*. *Anal. Biochem.* **314**:235-242.
15. **Hollis, T., Ichikawa, Y., and Ellenberger, T.** 2000. DNA bending and a flip-out mechanism for base excision by the helix-hairpin-helix DNA glycosylase, *Escherichia coli* AlkA. *The EMBOJournal* **19**:758-66.
16. **Ikeda, Y., K. Okamura-Ikeda, and K. Tanaka.** 1985. Spectroscopic analysis of the interaction of rat liver short-chain, medium-chain, and long-chain acyl coenzyme A dehydrogenases with acyl coenzyme A substrates. *Biochemistry* **24**:7192-7199.
17. **Imlay, J. A.** 2003. Pathways of oxidative damage. *Annu. Rev. Microbiol.* **57**:395-418.
18. **Jaroszewski, L., L. Rychlewski, Z. Li, W. Li, and A. Godzik.** 2005. FFAS03: A server for profile-profile sequence alignment. *Nucl. Acids Res.* **33**.
19. **Jeffery, A. M.** 1985. DNA modification by chemical carcinogens. *Pharmacology and Therapeutics.* **28**:237-72.
20. **Jeggo, P.** 1979. Isolation and characterization of *Escherichia coli* K-12 mutants unable to induce the adaptive response to simple alkylating agents. *J. Bacteriol.* **139**:783-91.
21. **Jing, D., J. Agnew, W. F. Patton, J. Hendrickson, and J. M. Beechem.** 2003. A sensitive two-color electrophoretic mobility shift assay for detecting both nucleic acids and protein in gels. *Proteomics* **3**:1172-1180.
22. **Jones, D. T.** 1999. Protein secondary structure prediction based on position-specific scoring matrices. *J. Mol. Biol.* **292**:195-202.
23. **Karplus, K., R. Karchin, C. Barrett, S. Tu, M. Cline, M. Diekhans, L. Grate, J. Casper, and R. Hughey.** 2001. What is the value added by human intervention in protein structure prediction? *Suppl. 5*.

24. **Khanna, P., and M. S. Jorns.** 2003. Tautomeric rearrangement of a dihydroflavin bound to monomeric sarcosine oxidase or *N*-methyltryptophan oxidase. *Biochemistry* **42**:864-869.
25. **Kim, J.J. P., and R. Miura.** 2004. Acyl-CoA dehydrogenases and acyl-CoA oxidases. Structural basis for mechanistic similarities and differences. *Eur. J. Biochem.* **271**:483-493.
26. **Koh, I. Y. Y., V. A. Eylich, M. A. Marti-Renom, D. Przybylski, M. S. Madhusudhan, N. Eswar, O. Grana, F. Pazos, A. Valencia, A. Sali, and B. Rost.** 2003. EVA: evaluation of protein structure prediction servers. *Nucl. Acids Res.* **31**:3311-3315.
27. **Koradi, R., M. Billeter, and K. Wüthrich.** 1996. MOLMOL: a program for display and analysis of macromolecular structures. *J. Molec. Graphics Modeling* **14**:51-55.
28. **Krokan, H. E., R. Standal, and G. Slupphaug.** 1997. DNA glycosylases in the base excision repair of DNA. *Biochem. J.* **325**:1-16.
29. **Lacour, S., Kolb, A., Landini, P.** 2003. Nucleotides from -16 to -12 Determine Specific Promoter Recognition by Bacterial σ^S -RNA Polymerase. *J. Biol. Chem.* **278**:37160-37168.
30. **Lacour, S., Leroy, O., Kolb, A., and Landini, P.** 2004. Substitutions in Region 2.4 of σ^{70} Allow Recognition of the S-Dependent *aidB* Promoter. **279**:55255-55261.
31. **Lacoura, S., Kolbb, A., Jakob, A., Zehndera, B., and Landini, P.** 2002. Mechanism of Specific Recognition of the *aidB* Promoter by σ^S -RNA Polymerase. *Biochem. Biophys. Res. Commun.* **292**:922-30.
32. **Laemmli, U. K.** 1970. Cleavage of structural proteins during the assembly of the head of bacteriophage T4. *Nature (London)* **227**:680-685.
33. **Landini, P., L. I. Hajec, and M. R. Volkert.** 1994. Structure and transcriptional regulation of the *Escherichia coli* adaptive response gene *aidB*. *J. Bacteriol.* **176**:6583-6589.
34. **Landini, P., and M. R. Volkert.** 2000. Regulatory responses of the adaptive response to alkylation damage: a simple regulon with complex regulatory features. *J. Bacteriol.* **182**:6543-6549.
35. **Landini, P., and M. R. Volkert.** 1995. Transcriptional activation of the *Escherichia coli* adaptive response gene *aidB* is mediated by binding of methylated Ada protein. *J. Biol. Chem.* **270**:8285-8289.

36. **Landry, J., and R. Sternglanz.** 2003. Yeast Fms1 is a FAD-utilizing polyamine oxidase. *Biochem. Biophys. Res. Commun.* **303**:771-776.
37. **Lenich, A. C., and S. I. Goodman.** 1986. The purification and characterization of glutaryl-coenzyme A dehydrogenase from porcine and human liver. *J. Biol. Chem.* **261**: 4090-4096.
38. **Massey, V., and P. Hemmerich.** 1980. Active site probes of flavoproteins. *Biochem. Soc. Trans.* **8**:246-257.
39. **Massey, V., and P. Hemmerich.** 1978. Photoreduction of flavoproteins and other biological compounds catalyzed by deazaflavins. *Biochemistry* **17**:9-16.
40. **Massey, V., F. Müller, R. Feldberg, M. Schuman, P. A. Sullivan, L. G. Howell, S. G. Mayhew, R. G. Matthews, and G. P. Foust.** 1969. The reactivity of flavoproteins with sulfite. Possible relevance to the problem of oxygen reactivity. *J. Biol. Chem.* **244**:3999-4006.
41. **Massey, V., M. Stankovich, and P. Hemmerich.** 1978. Light-mediated reduction of flavoproteins with flavins as catalysts. *Biochemistry* **17**:1-8.
42. **Matijasevic, Z., L. I. Hajec, and M. R. Volkert.** 1992. Anaerobic induction of the alkylation-inducible *Escherichia coli aidB* gene involves genes of the cysteine biosynthetic pathway. *Journal of Bacteriology* **174**:2043-2046.
43. **Matsudaira, P.** 1987. Sequence from picomole quantities of proteins electroblotted onto polyvinylidene difluoride membranes. *J. Biol. Chem.* **262**:10035-10038.
44. **McGuffin, L. J., K. Bryson, and D. T. Jones.** 2000. The PSIPRED protein structure prediction server. *Bioinformatics* **16**:404-405.
45. **Miroux, B., and J. E. Walker.** 1996. Over-production of proteins in *Escherichia coli*: mutant hosts that allow synthesis of some membrane protein and globular proteins at high levels. *J. Mol. Biol.* **260**:289-298.
46. **Mohsen, W.-W. A., B. D. Anderson, S. L. Volchenboun, K. P. Battaile, K. Tiffany, D. Roberts, J.-J. Kim, and J. Vockley.** 1998. Characterization of molecular defects in isovaleryl-CoA dehydrogenase in patients with isovaleric acidemia. *Biochemistry* **37**:10325-10335.
47. **Nagpal, A., M. P. Valley, P. F. Fitzpatrick, and A. M. Orville.** 2004. Crystallization and preliminary analysis of active nitroalkane oxidase in three crystal forms. *Acta Crystallogr D Biol Crystallogr* **60**.

48. **Nakajima, Y., I. Miyahara, K. Hirotsu, Y. Nishima, K. Shiga, C. Setoyama, H. Tamaoki, and R. Miura.** 2002. Three-dimensional structure of the flavoenzyme acyl-CoA oxidase II from rat liver, the peroxisomal counterpart of mitochondrial acyl-CoA dehydrogenase. *J. Biochem.* **131**:365-374.
49. **New York Academy of Sciences, e. b. S. S. W., Bennett van Houten, and Yoke Wah Kow.** 1994. DNA damage : effects on DNA structure and protein recognition. *Annals of the New York Academy of Science* **726**.
50. **Nicholls, A., K. Sharp, and B. Honig.** 1991. Protein folding and association: insights from the interfacial and thermodynamic properties of hydrocarbons. *Proteins: Struct. Funct. Genet.* **11**:281-296.
51. **Olsson, M., T. Lindhal.** 1980. Repair of alkylated DNA in Escherichia coli. Methyl group transfer from O6-methylguanine to a protein cysteine residue. *J. Biol. Chem.* **255**:10569-10571.:10569-10571.
52. **Ouyang, T., and D. R. Walt.** 1991. A new chemical method for synthesizing and recycling acyl coenzyme A thioesters. *J. Org. Chem.* **56**:3752-3755.
53. **Parker, B. O. a. M. G. M.** 1992. Repair of DNA heteroduplexes containing small heterologous sequences in Escherichia coli. *Proc. Natl. Acad. Sci. USA* **89**:1730-4.
54. **Peak, M. J., Peak, J. G., Balzek, A.R.** 1988. Radiation-induced DNA damage and repair: Argonne National Laboratory Symposium. *International Journal of Radiation Biology* **54**:563-6.
55. **Rost, B.** 2001. Review: Protein secondary structure prediction continues to rise. *J. Struct. Biol.* **134**:204-218.
56. **Samson, L. D. a. C., J.** 1977. A new pathway for DNA repair in Escherichia coli. *Nature* **267**.:281-3.
57. **Sedgwick, B., and T. Lindahl.** 2002. Recent progress on the Ada response for inducible repair of DNA alkylation damage. *Oncogene* **21**:8886-8894.
58. **Shi, Y., F. Lan, C. Matson, P. Mulligan, J. R. Whetstine, P. A. Cole, R. A. Casero, and Y. Shi.** 2004. Histone demethylation mediated by the nuclear amine oxidase homolog LSD1. *Cell* **119**:941-953.
59. **Simrnova, G. V., Oktyabrsky, O. N., Moshonkina, F. V., Zakirova, N. V.** 1994. Induction of the alkylation-inducible aidB gene of Escherichia coli by cytoplasmic acidification and N-ethylmaleimide. *Mutat Res.* **314**:51-56.

60. **Teo, I., Sedgwick, B., Kilpatrick, M.W., McCarthy, T.V., Lindhal, T.** 1986. The intracellular signal for induction of resistance to alkylating agents in *E. coli*. *Cell* **42**:315-24.
61. **Trewick, S. C., T. F. Henshaw, R. P. Hausinger, T. Lindahl, and B. Sedgwick.** 2002. Oxidative demethylation by *Escherichia coli* AlkB directly reverts DNA base damage. *Nature* **419**:174-178.
62. **Visse, R., et al.** 1992. Analysis of UvrABC endonuclease reaction intermediates on cisplatin-damaged DNA using mobility shift gel electrophoresis. *J. Biol. Chem.* **267**:6736-42.
63. **Volkert, M. R.** 1988. Adaptive response of *Escherichia coli* to alkylation damage. *Environ. Mol. Mutagen.* **11**:241-255.
64. **Volkert, M. R., F. H. Gately, and L. I. Hajec.** 1989. Expression of DNA damage-inducible genes of *Escherichia coli* upon treatment with methylating, ethylating and propylating agents. *Mut. Res.* **217**:109-115.
65. **Volkert, M. R., L. I. Hajec, and D. C. Nguyen.** 1989. Induction of the alkylation-inducible *aidB* gene of *Escherichia coli* by anaerobiosis. *J. Bacteriol.* **171**:1196-1198.
66. **Volkert, M. R., L. L. Hajec, and Z. Matiasovic.** 1994. Anaerobic induction of the *Escherichia coli* *aidB* gene requires a functional *rpoS* (*katF*) gene. *J. Bacteriol.* **176**:7638-45.
67. **Volkert, M. R., and D. C. Nguyen.** 1984. Induction of specific *Escherichia coli* genes by sublethal treatments with alkylating agents. *Proc. Natl. Acad. Sci. USA* **81**:4110-4114.
68. **Volkert, M. R., D. C. Nguyen, and K. C. Beard.** 1986. *Escherichia coli* gene induction by alkylation treatment. *Genetics* **112**:11-26.
69. **Watanabe, K., C. Khosla, R. M. Stroud, and S.C. Tsai.** 2003. Crystal structure of an acyl-ACP dehydrogenase from the FK520 polyketide biosynthetic pathway: insights into extender unit biosynthesis. *J. Mol. Biol.* **334**:435-444.
70. **Wei, Y.F., K. C. Carter, R.-P. Wang, and B. K. Shell.** 1996. Molecular cloning and functional analysis of a human cDNA encoding an *Escherichia coli* AlkB homolog, a protein involved in DNA alkylation damage repair. *Nucl. Acids Res.* **24**:931-937.

MICHIGAN STATE UNIVERSITY LIBRARIES



3 1293 02736 6883